

## Enhanced Super Capacitor Performance of WO<sub>3</sub> Nano Crystals by Doping Cadmium-Metal Ions

<sup>1</sup>S.Kalaiarasi, <sup>2</sup>R.R.Muthuchudarkodi, <sup>3</sup>C.StellaPackiam and <sup>4</sup>S.Maheswari

<sup>1</sup>Research scholar, Reg. No. 18222232032025, Department of Chemistry, V.O. Chidambaram College, Thoothukudi, Affiliated to Manonmaniam Sundarnar University, Tirunelveli

<sup>1,3,4</sup> Department of Chemistry, A.P.C.Mahalaxmi College, Thoothukudi

<sup>2</sup>PG and Research Department of Chemistry, V.O. Chidambaram College, Thoothukudi

### Abstract

In this paper, we present a general approach for the preparation of Cadmium ion-doped WO<sub>3</sub> nanoparticles. This study presents the preparation of tungsten trioxide (WO<sub>3</sub>) nanoparticles by using sodium tungstate as a precursor. Cadmium ion-doped WO<sub>3</sub> nanoparticles were successfully prepared by the chemical Co-precipitation method. The synthesized samples were characterized by relevant characterization techniques such as FT-IR (Identification of functional groups), scanning electronic microscopy (crystal structure, morphology). FTIR confirms the presence of respective functional groups. Then SEM images indicate surface morphology for the prepared samples. To access the properties of WO<sub>3</sub> nanoparticles for their use in supercapacitors, cyclic voltammetry and EIS (Electro Chemical Impedance Spectroscopic) measurements are performed. Cadmium ion-doped WO<sub>3</sub> nanocrystals exhibit a maximum specific capacitance of 136 Fg<sup>-1</sup> at a scan rate of 50mVs<sup>-1</sup>. These doped WO<sub>3</sub> nanoparticles could be a promising candidate material for high capacity, low-cost, and environmentally friendly electrodes for supercapacitors.

**Key Words:** FTIR, SEM, Cyclic Voltammetry, supercapacitors, Nanocrystals

### 1. Introduction

Nanotechnology is creating a growing sense of excitement in life sciences especially biomedical devices and biotechnology [1]. Nanoparticles are routinely defined as microscopic particles with sizes between 1 nm and 100 nm that show properties that are not found in bulk samples of the same material [2]. In this size range, the physical, chemical, and biological properties of the nanoparticles changes in fundamental ways from the properties of both individual atoms/molecules and of the corresponding bulk materials. Nanoparticles can be made of materials of diverse chemical nature, the most common being metals, metal oxides, silicates, non-oxide ceramics, polymers, organics, carbon, and biomolecules. Nanoparticles exist in several different morphologies such as spheres, cylinders, platelets, tubes, etc. Generally, the nanoparticles are designed with surface modifications tailored to meet the needs of specific applications they are going to be used for. The enormous diversity of the nanoparticles arising from their wide

chemical nature, shape, and morphologies, the medium in which the particles are present, the state of dispersion of the particles and most importantly, the numerous possible surface modifications the nanoparticles can be subjected to make this an important active field of science nowadays.

Tungsten Oxide ( $\text{WO}_3$ ) is one of the most sought-after materials for material researchers and shows photochromic, electrochromic, and gaschromic properties[3].  $\text{WO}_3$  has been extensively studied in recent years due to its widespread applications in smart windows, non-emissive displays, optical signal processing, sensors, information storage media, etc. The most stable  $\text{WO}_3$  at room temperature has a monoclinic structure. Because of its electrochromic and photochromic applications, most of the studies of this material are in the thin film form and studies on nanocrystalline samples of  $\text{WO}_3$  in powder form are rather limited. Here an attempt has been made to synthesize nanocrystalline  $\text{WO}_3$  in a fine powder form with different average crystalline sizes by employing a controlled chemical precipitation method.

Cadmium (Cd) is a naturally occurring metal situated in the Periodic Table of the Elements between zinc (Zn) and mercury (Hg), with chemical behavior similar to Zn. It generally exists as a divalent cation, complexed with other elements (e.g.,  $\text{CdCl}_2$ ). Cd exists in the earth's crust at about 0.1 parts per million, usually being found as an impurity in Zn or lead (Pb) deposits, and therefore being produced primarily as a byproduct of Zn or PbS melting. Commercially, Cd is used in television screens, lasers, batteries, paint pigments, cosmetics, and galvanizing steel, as a barrier in nuclear fission, and was used with zinc to weld seals in lead water pipes before the 1960s. Approximately 600 metric tons are produced annually in the United States and about 150 metric tons are imported [4].

Supercapacitors have attracted growing interest, due to their high power density, long cycle life, and fast charging rate, which is playing an important role in complementing or even replacing batteries in many applications [5]. Supercapacitors are also known as electrochemical capacitors have been a subject to many applications, research, and development due to their high power density, environmental friendliness, long shelf life, long life cycle [6-8] and it bridges the energy gap between capacitors (high power output) and fuel cells/batteries (high energy storage)[9,10]. In this work, we synthesized and characterized nanocrystals by FTIR, SEM, and Cyclic Voltammetry Studies. Surface functional groups were identified using FT-IR analysis. The present communication reports a cyclic voltammetric study in understanding the electrochemical behavior of  $\text{WO}_3$  and cadmium ion-doped  $\text{WO}_3$  nanoparticles. The electrochemical response and the charge storage capability of these nanoparticles had also been investigated.

## 2. Experimental

### Materials and Methods

Sodium Tungstate, Concentrated Hydrochloric Acid, Cadmium chloride, and deionized water was as used to synthesize WO<sub>3</sub> nanoparticles and cadmium ion-doped WO<sub>3</sub> nanoparticles.

#### 2.1. Synthesis of Undoped WO<sub>3</sub> Nanoparticles

WO<sub>3</sub> nanoparticles were synthesized at room temperature by the chemical Co-precipitation method. WO<sub>3</sub> nanoparticles were synthesized by using sodium tungstate as the precursor material. All the reagents used were of analytical grade and, used without further purification. The entire process was carried out in deionized water for its inherent advantages of being simple and environment friendly. In a typical preparation, a solution of 0.1M sodium tungstate was prepared in 100ml of deionized water and then an aqueous solution of (100ml, 1M) hydrochloric acid was added dropwise to this solution making a final volume of 200ml. This mixture was stirred well for 1h and refluxed at a temperature of about 80°C which resulted in the formation of green-colored WO<sub>3</sub> nanoparticles. The precipitate was separated from the reaction mixture, washed several times with deionized water to remove the impurities. The precipitate was dried at room temperature.

#### 2.2. Synthesis of Cadmium Ion-doped WO<sub>3</sub> Nanoparticles

Cadmium ion-doped WO<sub>3</sub> nanoparticle was prepared at room temperature by the chemical Co-precipitation method. To a 100ml of 0.1M solution of sodium tungstate, hydrochloric acid solution(100 ml of 1M) was added in drops. The resulting solution was stirred for 30 minutes. It resulted in a yellow-colored solution. Then CdCl<sub>2</sub>.2H<sub>2</sub>O in (100ml in 0.1M) deionized water was added to the above solution. The resulting solution was stirred for about 30 min and this solution was refluxed for 3 h at a temperature of about 80°C which resulted in the formation of Cd ion-doped WO<sub>3</sub> nanoparticles. The precipitate so obtained was filtered and the filtrate was washed several times with distilled water to remove the impurities. The precipitate was dried at room temperature[11].

## 3. Characterization

The FT-IR spectra were recorded using a SHIMADZU instrument. FESEM measurements are carried by JEOL JSM-6700F field emission scanning electron microscope. The electrochemical behavior of metal oxide nanoparticles have been investigated through CHI-650 Chemical Workstation Instrument Inc., TX, USA.

## 4. Result and Discussion

### 4.1. Functional Group Analysis

FT-IR spectra of undoped and doped nanoparticles were recorded in the range of 400-4000 $\text{cm}^{-1}$ . Fig.1 shows the FT-IR spectra of undoped and doped nanoparticles. Fig:1a showed a characteristic peak at 1383.85 $\text{cm}^{-1}$  which is assigned to the O2 stretching frequency of nano  $\text{WO}_3$  [12]. In addition, there is a peak at 1464.63  $\text{cm}^{-1}$  that corresponds to the O-H bending of the hydroxyl group present[13]. The absorption band in the region of 668.87 $\text{cm}^{-1}$  is assigned to W–O stretching vibration mode [14]. The absorption of  $\text{CO}_2$  from the atmosphere at the WO surface was identified from the sharp peak positioned at about 1620.70  $\text{cm}^{-1}$  in FTIR spectra. The broad absorption band centered at 3397.52  $\text{cm}^{-1}$  is assigned to H – O – H bending vibrations mode which were also presented due to adsorption of water in the air[15].

FT-IR spectra of Cd ion-doped  $\text{WO}_3$  metal oxide nanoparticles are shown in (Fig.1b) Cd ion-doped  $\text{WO}_3$  metal oxide nanoparticles exhibit a broad absorption band in the range of 3438 $\text{cm}^{-1}$  is assigned to the O–H stretching vibration and indicating the presence of hydroxyl groups[16]. The peaks at 1621.20  $\text{cm}^{-1}$  are due to -C-H- stretching. The band at 1384.44  $\text{cm}^{-1}$  can be attributed to the aromatic -C=C- bond. The peak observed at around 668.07  $\text{cm}^{-1}$  indicating the formation of stretching mode of Cd ion-doped  $\text{WO}_3$  nanoparticles[17]. These functional groups indicate the presence of both Cd ion and Tungsten oxide in the doped sample.

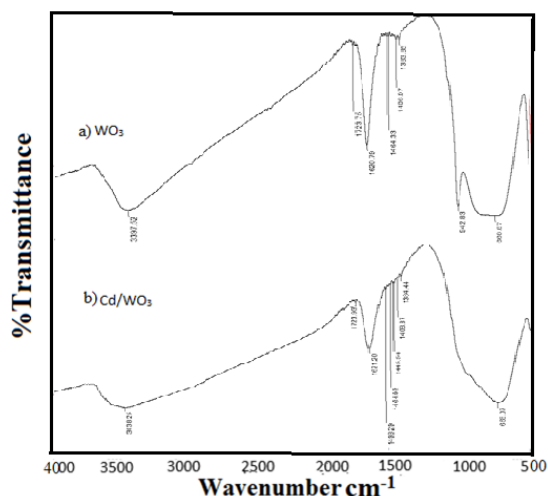


Fig:1 FT-IR Spectra of a)Undoped  $\text{WO}_3$  nanoparticles b) Cd ion-doped  $\text{WO}_3$  nanoparticles

### 4.2. Morphological Study

Surface morphologies of undoped WO<sub>3</sub> nanoparticles and Cd ion-doped WO<sub>3</sub> doped nanoparticles are investigated by FESEM as shown in Fig.2. The morphology of Cd ion-doped samples is different from undoped samples. The surface morphologies of synthesized WO<sub>3</sub> nanoparticles (Fig.2a) exhibited a square-like structure[18]. For the undoped sample, only aggregates are formed whereas, for the Cd ion-doped WO<sub>3</sub> nanoparticles, the FESEM image shows that irregularly shaped nanoparticles (Fig.2b) are well separated[19]. Surface morphologies of undoped WO<sub>3</sub> nanoparticles and Cd ion-doped WO<sub>3</sub> doped nanoparticles are the same size but different magnifications.

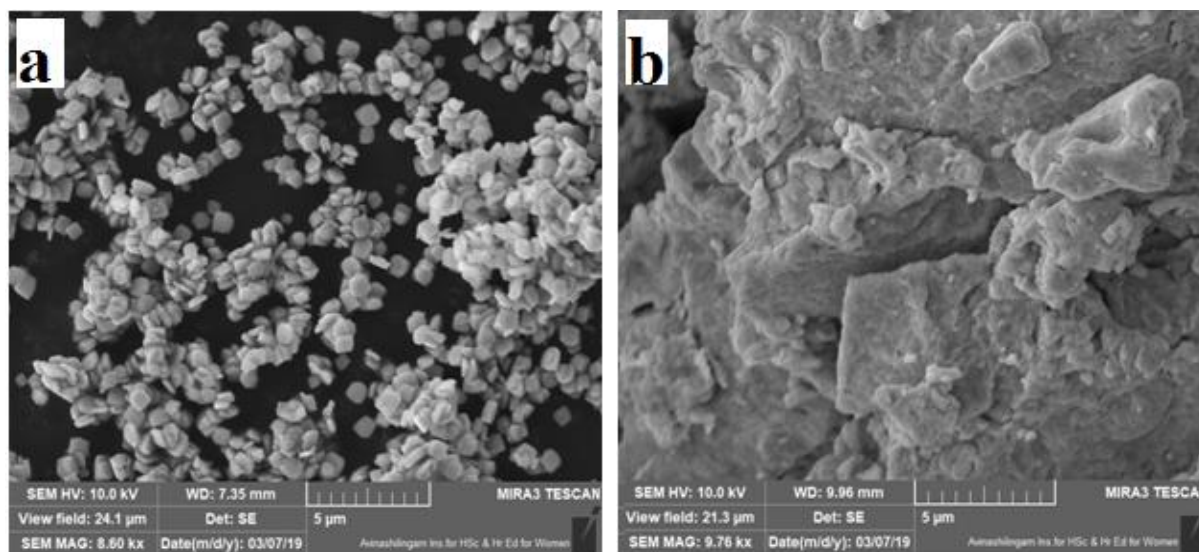


Fig:2 FESEM images of a) undoped WO<sub>3</sub> nanoparticles b) Cd ion-doped WO<sub>3</sub> nanoparticles

### 4.3. Cyclic Voltammetric Studies

The cyclic voltammetric measurements were performed to evaluate the electrochemical behavior of the electrodes between -0.6 and 0.12 V in 0.1 M KOH. Fig. 3 shows the CV curves of WO<sub>3</sub> nanoparticles measured at different scan rates of 50,75,100 and 125mVs<sup>-1</sup> in 0.1MKOH aqueous electrolyte[20]. Cyclic voltammetric behavior of WO<sub>3</sub> nanoparticles showed one oxidation peak at 0.2821 V as shown in Fig.3.

Cyclic voltammetric behavior of Cd ion-doped WO<sub>3</sub> nanoparticles showed one oxidation peak at 0.2702V as shown in Fig.4[21]. This lower current rate indicates an efficient diffusion of hydroxyl ions into the electrode, thereby clearly revealing the electrochemical processes. The CV curves of all electrodes at various scan rates are given in the supplementary information [20].

The specific capacitance can be calculated from the CV curve using the following equations

$$= \frac{\int ivdv}{2\mu m\Delta V}$$

where  $i$  and  $v$  are the current and potential in the CV curve (A and V),  $\mu$  is the scan rate (V/s),  $m$  is the mass of active materials (g) and  $\Delta V$  is the potential window[22].

The cyclic voltammetry process was carried out to observe the electrochemical performance of the synthesized  $\text{WO}_3$  nanoparticles and Cd ion-doped  $\text{WO}_3$  nanoparticles for supercapacitor applications. The capacitance behavior of the nanoparticles was observed by the presence of anodic and cathodic peaks. This is further confirmed that the surface redox reactions have been taken place[23]. Fig.5 shows that the variation in the specific capacitance of doped and undoped samples modified GCE as a function of scan rates. It could be found that the specific capacitance decreases with the increase of scan rates from 50 to 125  $\text{mVs}^{-1}$ . The specific capacitance value obtained for the undoped  $\text{WO}_3$  and Cadmium ion-doped  $\text{WO}_3$  nanoparticles were 122 F/g and 136 F/g at a 50  $\text{mVs}^{-1}$  scan rate. The decrease of specific capacitance with increasing the scan rates is due to the relatively long diffusion length for the structure of the prepared samples and an increase of the ion transport-related resistance[24].

A lower specific capacitance was observed using a higher scan rate due to reduced charge storage capacity. This is expected for a higher scan rate as the electrolyte ions could not enter inside the interior part of the electrode materials. The minimum area of the electrode was used by the electrolyte ions at a lower scan rate. This resulted in superior values for specific capacitance. Moreover, the electrochemical capacitive behavior depends on the rate of charge exchange. This depends on the diffusion of anions and cations towards the electrode/electrolyte interfaces. The specific capacitance values are inversely proportional to the scan rate. At a lower scan rate, positive ions can simply diffuse inside every accessible site of materials. This initiates satisfactory insertion pathways for reaction. However, at a higher scan rate, positive ions can approach the only outer surface of the electrode. The constituent materials found inside the inward space have a minor role in capacitance behavior. This initiates a slight deviation from ideality and fewer capacitance values[23].

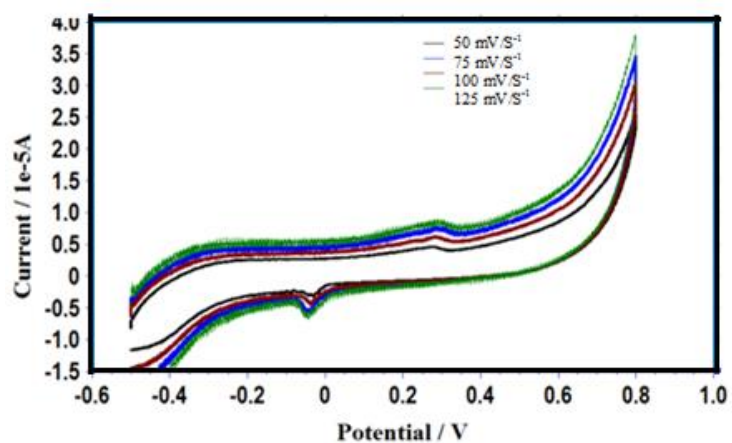


Fig:3 Cyclic voltammetric behaviour of undoped WO<sub>3</sub> nanoparticles at different scan rates

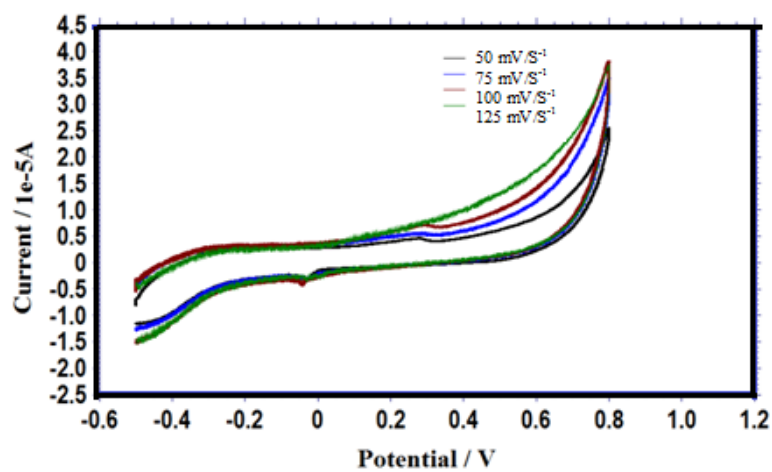


Fig:4 Cyclic voltammetric behaviour of Cd ion-doped WO<sub>3</sub> nanoparticles at different scan rates

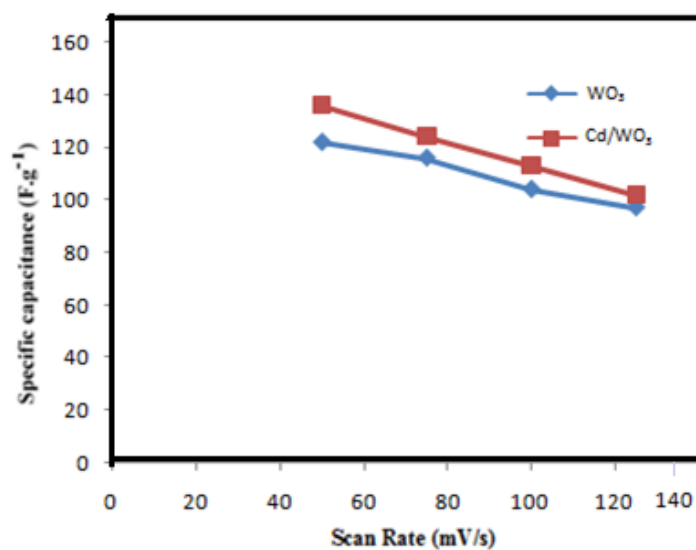


Fig 5: Plot of scan rate verses specific capacitance for nano WO<sub>3</sub> and Cd ion-doped WO<sub>3</sub> nanoparticles

#### 4.4. Electrochemical Impedance Study

Electrochemical impedance analysis is an informative technique to evaluate the properties of conductivity and charge transport in the electrode/electrolyte interface. Therefore, the electrochemical properties of undoped WO<sub>3</sub> and Cd ion-doped WO<sub>3</sub> nanoparticles were evaluated using EIS techniques. The impedance measurements were performed in the presence of 0.1MKOH with as an amplitude at scanning frequency range from 100000Hz to 0.01Hz.

The Nyquist plots for GCE and all modified electrodes in 0.1MKOH. The impedance spectra of undoped WO<sub>3</sub> and Cd ion-doped WO<sub>3</sub> nanoparticles are shown in Fig:6a and 6b. Table:1 shows the Cdl values of undoped WO<sub>3</sub> and Cd ion-doped WO<sub>3</sub> nanoparticles. In the low-frequency region, the impedance plot is increased sharply and tends to become vertical which is due to the capacitive nature of the electrode. The intercept of higher frequency on the X-axis yields the electrolyte resistance (Rs) and the diameter of the semicircle yields the charge transfer resistance (Rct)[25]. A large charge transfer resistance was observed for Cd ion-doped WO<sub>3</sub> nanoparticles than WO<sub>3</sub> nanoparticles which is due to the excellent conductivity.

Table:1 shows the Rct and Cdl values of undoped WO<sub>3</sub> and Cd ion-doped WO<sub>3</sub> nanoparticles. The decrease in Cdl is attributed to an increase in thickness of the electronic double layer in ion-doped samples. The increase in Rct value is attributed to the decrease of Cdl values of undoped WO<sub>3</sub> and Cd ion-doped WO<sub>3</sub> nanoparticles. The increase in Rct value is attributed to the formation of protective film on the metal/solution interface[26]. The lower Rct value of the WO<sub>3</sub> nanoparticles leads to improved charge transfer and enhanced capacitance[27]. EIS plot with a semicircle and a linear portion corresponding to a charge transfer and mass transportation procedure at the high-frequency region and the low-frequency region, respectively[28].



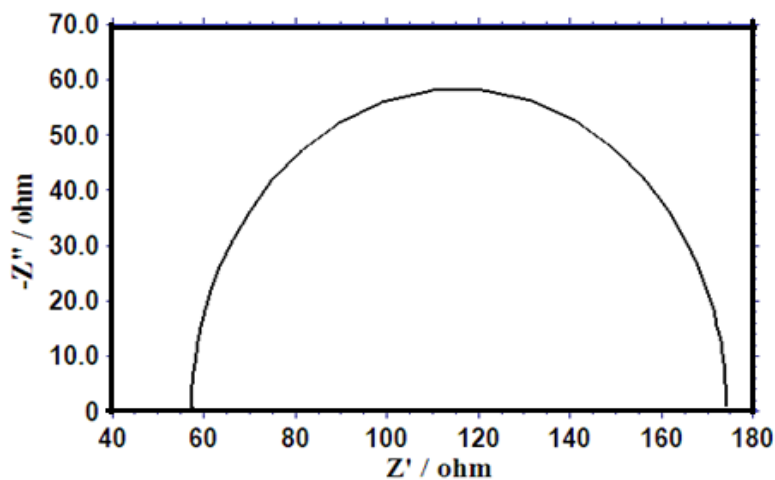


Fig:6a Electrochemical Impedance spectra of undoped WO<sub>3</sub> nanoparticles

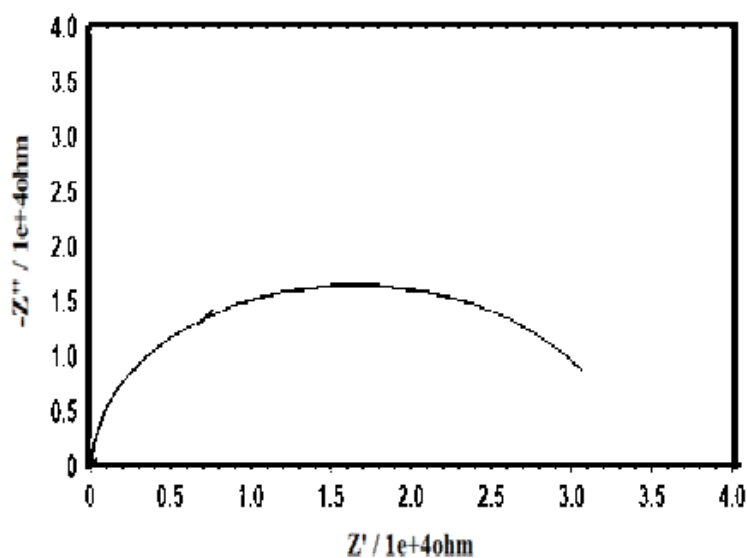


Fig:6b Electrochemical Impedance spectra of Cd ion-doped WO<sub>3</sub> nanoparticles

**Table:1 R<sub>s</sub>, R<sub>ct</sub> and C<sub>dl</sub> values of undoped WO<sub>3</sub> and Cd ion-doped WO<sub>3</sub> nanoparticles**

Samples	R <sub>s</sub>	R <sub>ct</sub> (Ω cm <sup>2</sup> )	C <sub>dl</sub> (μF cm <sup>-2</sup> )
WO <sub>3</sub> Nanoparticles	57.98	116.9	0.1245 x e <sup>-3</sup>
Cadmium ion-doped WO <sub>3</sub> Nanoparticles	165.20	3061	0.0317 x e <sup>-3</sup>

#### 4.4. Super Capacitive Behaviour -Bode Plot

Fig.7 and Fig.8 illustrated the analogous trend found in Bode magnitude and Bode phase angle plots of nanoWO<sub>3</sub> and Cd ion-doped WO<sub>3</sub> nanoparticles. The phase angle  $\theta$  can vary between 90° (for a perfect capacitor  $n = 1$ ) to 0° (for a perfect resistor  $n = 0$ ) [19]. The value of  $n$  is obtained from the slope of frequency versus the  $|Z|$  plot. Bode plot (-phase angle (degree) vs. log f(Hz) shown in Fig.7a, the bode phase angle for Cd ion-doped WO<sub>3</sub> nanoparticles is 97°. Bode plot (-phase angle (degree) vs. log f(Hz) shown in Fig.7b, the bode phase angle for nanoWO<sub>3</sub> is closed to 79° lower than that for Cd ion-doped WO<sub>3</sub> nanoparticles (97°), exhibits Cd ion-doped WO<sub>3</sub> nanoparticles better supercapacitor behavior than tungsten oxide(WO<sub>3</sub>) nanoparticles. The Bode phase angle plot shows the change in phase angle concerning the applied frequency. From Fig.7b, it is evidenced that the phase angle is nearly 79° which further confirms the pseudocapacitive nature of the tungsten oxide modified electrodes[29].

From the bode plot as shown in Fig.8a, at the low-frequency region, the slope values for Cd ion-doped WO<sub>3</sub> nanoparticles is 0.5 ( $R_2=1$ ), which indicates the characteristic of a supercapacitor. The plot of log  $|Z|$  versus log f (Hz)(Fig.8b) also gave a slope value in the range of 0.9 ( $R_2 = 1.000$ ) suggesting the pseudocapacitive behavior of nano Tungsten oxide [29]. These results suggest that the behavior of the doped sample modified electrode changes from a pure resistor at high frequency to pseudo capacitors at low frequency. The maximum phase angle has been achieved for Cd ion-doped WO<sub>3</sub> coated GCE compared to the nano WO<sub>3</sub> coated glassy carbon electrode[30].

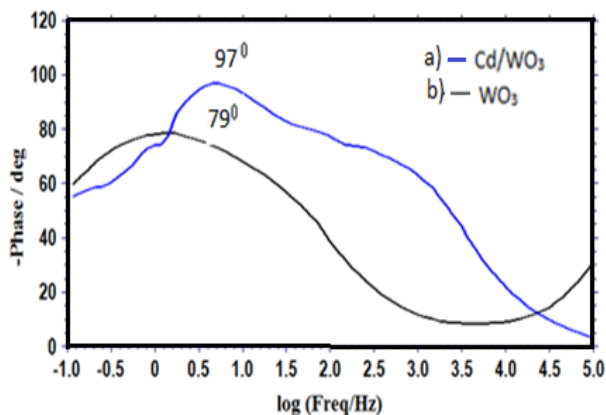


Fig.7 Bode plot of -phase angle/ deg. versus log (f/Hz)) for a) Cd ion-doped WO<sub>3</sub> nanoparticles  
b) WO<sub>3</sub> nanoparticles

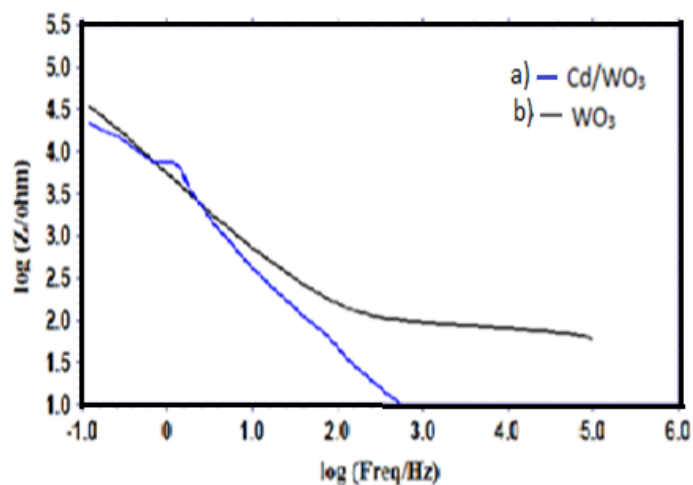


Fig:8 Bode plot of  $\log |Z|/\text{ohm}$  versus  $\log (f/\text{Hz})$  for a) Cd ion-doped WO<sub>3</sub> nanoparticles b) WO<sub>3</sub> nanoparticles

## 5. Conclusion

Nano WO<sub>3</sub> and Cd ion-doped WO<sub>3</sub> nanoparticles were synthesized using the chemical co-precipitation method. The characterization of prepared samples was characterized by FTIR, FESEM, and electrochemical studies. FT-IR spectral results revealed that the presence of M-O bonds of the synthesized nanoparticles. Surface morphological features with particle size and shape were confirmed by FESEM analysis. Cyclic voltammetry results show a maximum specific capacitance of 136 F/g for Cd ion-doped WO<sub>3</sub> nanoparticles at a 50 mV/s scan rate. EIS measurements show that the lower R<sub>ct</sub> value of the WO<sub>3</sub> nanoparticles leads to improved charge transfer and enhanced capacitance. The maximum phase angle has been achieved for Cd ion-doped WO<sub>3</sub> nanoparticles compared to the WO<sub>3</sub> nanoparticles. It indicates the characteristic of a supercapacitor.

## Acknowledgement

The authors are thankful to The Secretary of A.P.C Mahalaxmi College for women, Thoothukudi for providing us the CHI-650 electro chemical workstation. We are also extremely grateful to PG and Research Department of Chemistry, V.O.Chidambaram College, Thoothukudi for providing us the SHIMADZU FTIR Spectrophotometer. s

## References

- [1]. Prabhu N, Divya TR, Yamuna G (2010), Synthesis of silver phyto nanoparticles and their antibacterial efficacy, *Digest J NanomatBiostruc* 9; pp:185.

- [2]. Melanie A, Jerome R, Jean BY, et al (2009), Towards a definition of inorganic nanoparticles from an environmental, health and safety perspective nature, *Nature Nanotechnology(PubMed)* 4:634-41.
- [3].Niklasson A G, Granqvist G( 2007), Electrochromics for smart windows: thin films of tungsten oxide and nickel oxide, and devices based on these, *J. Mater. Chem* 17: 127.
- [4].HansWedepohl K (1995), The composition of the continental crust, *Geochimica et CosmochimicaActa*, vol. 59, no. 7: pp. 1217–1232.
- [5].Rusi and Majid R S (2015), Green synthesis of *in situ* electrodeposited rGO/MnO<sub>2</sub> nanocomposite for high energy density supercapacitors,*Scientific Reports (PubMed)* Nov 5;5:16195. doi: 10.1038/srep16195.
- [6].Ejikeme Raphael Ezeigwe, Michelle T T (2015),One-step green synthesis of graphene/ZnOnanocomposites for electrochemical capacitors,*Ceramics International* 41:715–724.
- [7]. Wang J, Gao Z, Li Z, Wang B, Yan Y, Liu Q, Mann T, Zhang M, Jiang Z (2011), Green synthesis of graphene nanosheets/ZnO composites and electrochemical properties, *J. Solid State Chem* 184:1421–1427.
- [8]. Baker J (2008).New technology and possible advances in energy storage, *Energy Policy* 36 : 4368–4373.
- [9].Wang G, Zhang L, Zhang J (2012), A review of electrode materials for electrochemical supercapacitors, *Chem. Soc. Rev.* 41: 797–828.
- [10].Bose S, Kuila T, Mishra K A, Rajasekar R, Kim H N, Lee H J (2012), Carbon-based nanostructured materials and their composites as supercapacitor electrodes, *J. Mater. Chem* 22: 767.
- [11].Heckert G E, Karakoti S A, Seal S, and Self T W (2008), The role of Cerium redox state in the SOD minetic activity of Nanoceria, *Biomaterials* 29: 2705.
- [12].NilofarAsima,Syuhami F M, MarziehBadiei and AmbarYarmo M (2014), WO<sub>3</sub> Modification by Synthesis of Nanocomposite, *Science Direct,NilofarAsim et al. / APCBEE Procedia* 9: 175 – 180.
- [13] Harish Kumar, Manisha and Poonam Sangwan(2013), Synthesis and Characterization of MnO<sub>2</sub>Nanoparticles using Co-precipitation Technique, *International Journal of Chemistry and Chemical Engineering*, Vol.No 3: pp. 155-160.
- [14]. Kanthimathi M., Dhathathreyan A. and Nair B.V (2004), Nanosized NiO using bovine serum albumin as template, *Mater. Lett* 58: 2914 – 2917.

- [15]. Liu K.C. and Anderson M.A (1996), Porous NiO/ Nickel films for electrochemical capacitors, *J. Electrochem. Soc* 143: 124-130.
- [16]. Farahmandjou M, Abaeiyan N (2017), Chemical Synthesis of Vanadium Oxide (V<sub>2</sub>O<sub>5</sub>) Nanoparticles Prepared by Sodium Metavanadate, *J. Nanomed Res* 5(1): 00103.
- [17]. Jay Chithra M, Sathya M, Pushpanathan K (2015), Effect of pH on Crystal Size and Photoluminescence Property of ZnO Nanoparticles Prepared by Chemical Precipitation Method, *Acta Metall. Sin.(Engl. Lett.)* 28:394-404.
- [18]. Li Z J, Yang B C, Zhang S R, Zhao C M (2012), Graphene oxide with improved electrical conductivity for supercapacitor electrodes, *Appl. Surf. Sci.*, 258: 3726-3731.
- [19]. Chidembo T A, Ozoemenas I K, Agboola O B, Gupta V, Wild goose G G, and Compton R G (2010), Electrochemical Capacitive Behaviour of Multiwalled Carbon Nanotubes Modified with Electropolymeric Films of Nickel Tetraaminophthalocyanine, *Energy Environ. Sci* 3: 228.
- [20]. Vidhyadharan B, Zain M K N, Misnon I I, Aziz A R, Ismail J, Yusoff M M, Jose R (2014), High performance supercapacitor electrodes from electrospun nickel oxide nanowires, *J. Alloy Compd* 610:14 3e150.
- [21]. Shyamala S, Muthuchudarkodi R R (April 2018), Polyindole Based Zinc Oxide Nanocomposite-Synthesis and Characterization, *International Journal of Science, Engineering and Management (IJSEM)*, Vol 3, Issue 4: 2456 -1304.
- [22]. Hulicova-Jurcakova D, Puziy A M, Poddubnaya I O, Suarez- Garcia F, Tascon D M J and Lu Q G, Am J(2009), Highly stable performance of supercapacitors from phosphorus-enriched carbons, *Journal of the American Chemical Society*, Apr 15;131(14):5026-7. doi: 10.1021/ja809265m.
- [23]. Suresh Sagadevana,b, Zaira Zaman Chowdhuryc, Mohd. Rafie Bin Johanc, Fauziah Abdul Aziza, Eme Marina Salleha, Anil Hawaa and Rahman F. Rafique (2018), A one-step facile route synthesis of copper oxide/reduced graphene oxide nanocomposite for supercapacitor applications, *Journal of experimental nanoscience* vol. 13, no. 1: 284–295. <https://doi.org/10.1080/17458080.2018.1542512>.
- [24]. Sathiyapriya A, Shameem Banu B I, Thirumalai J, Alagar A, March – April(2013), Optical characterization of Mn doped CdS nanoparticles synthesized by simple chemical route, *Optoelectronics And Advanced Materials – Rapid Communications* Vol. 7, No. 3-4: p. 191 – 195.

- [25]. Gund S G, Dubal P D, Patil H B, Shinde S S, Lokhande D C (2013), Enhanced activity of chemically synthesized hybrid graphene oxide/Mn<sub>3</sub>O<sub>4</sub> Composite for high performance supercapacitors, *Electrochim. Acta* 92 : 205-215.
- [26]. MuruganSaranya, RajendranRamachandran, FeiWang (2016), Graphene- Zinc oxide (G-ZnO) nanocomposite for Electrochemical Supercapacitor Applications, *Adv. Mater.Devic* 16: 2468-2179.
- [27]. Minoh Lee<sup>1\*</sup>, Suresh Kannan Balasingam<sup>2\*</sup>, Hu Young Jeong<sup>3</sup>, Won G. Hong<sup>4</sup>, Han-Bo-Ram Lee<sup>5</sup>, Byung Hoon Kim<sup>6</sup> & Yongseok 30 January (2015), One-step hydrothermal synthesis of graphene decorated V<sub>2</sub>O<sub>5</sub> nanobelts for enhanced electrochemical energy storage, *Scientific reports American Chemical society, Jan 30*.
- [28]. Halder, Arnab; Zhang, Minwei; Chi, Qijin (2016), Electrocatalytic Applications of Graphene–Metal Oxide Nanohybrid Materials, *Advanced Catalytic Materials Link to article, Feb 3 DOI:10.5772/61808*.
- [29]. Chung Jung Hung, Jeng Han Hung, Pang Lin, Tseung Yuen Tseng (2011), Electrophoretic Fabrication and Characterizations of Manganese Oxide/Carbon Nanotube Nanocomposite Pseudocapacitors, *Journal of The Electrochemical Society* 158(8): A942.
- [30]. Kallappa Deepa and Thimmappa Venkatarangaiah Venkatesha (2018), Synthesis of NiO-ZrO<sub>2</sub> Mixed Metal Oxide Nanoparticles and their Application in Zn-composite Coating on Mild Steel, *Anal.Bioanal.Electrochem* Vol. 10, No. 7: 890-900.